Available online at www.sciencedirect.com
SCIENCE DIRECT®
PERGAMON
Polyhedron 22 (2003) 1795–1801
POLYHEDRON
www.elsevier.com/locate/poly

Synthesis, crystal structure and magnetic properties of novel Mn_{12} single-molecule magnets with thiophenecarboxylate, $[Mn_{12}O_{12}(O_2CC_4H_3S)_{16}(H_2O)_4]$, and its tetraphenylphosphonium salt

Takayoshi Kuroda-Sowa [a,*], Tadahiro Nogami [a], Hisashi Konaka [a], Masahiko Maekawa [a], Megumu Munakata [a], Hitoshi Miyasaka [b], Masahiro Yamashita [b]

[a] Department of Chemistry, Faculty of Science and Engineering, Kinki University, Higashi-Osaka, Osaka, Japan
[b] Department of Chemistry, Faculty of Science, Tokyo Metropolitan University, Minami-Osawa, Hachioji, Tokyo 192-0397, Japan

Received 6 October 2002; accepted 31 December 2002

Abstract

The preparation and physical characterization are reported for novel Mn_{12} single-molecule magnets having thiophenecarboxylate bridges, $[Mn_{12}O_{12}(O_2CC_4H_3S)_{16}(H_2O)_4]$ (**1**), and its PPh_4 salt (**2**). The reaction of the excess amount of 2-thiophenecarboxylic acid (tpcH) and $[Mn_{12}O_{12}(OAc)_{16}(H_2O)_4]$ in CH_2Cl_2 gave black crystals of **1**, which could be reduced by PPh_4I to give **2**. From the crystal structure analysis of **2**, it is revealed that there are two five-coordinated Mn ions, one of which is assigned to a Mn^{II} ion being in the vicinity of the tetraphenylphosphonium cation. Both complexes exhibit out-of-phase a.c. magnetic susceptibility (χ''_M) signals in the 5.0–6.5 K range at 997 Hz a.c. frequency, which indicate that they are single-molecule magnets. From Arrhenius plots of the frequency dependence of the temperature of the χ''_M peaks, the effective energy barriers U_{eff} were estimated to be 69 and 57 K for high-temperature phases of **1** and **2**, respectively, and 40 K for the low-temperature phase of **1**. The reduced magnetization measurement and its analysis indicate that **2** has $S = 19/2$ ground state with $g = 1.99$ and $D = -0.61$ K.

Keywords: Single-molecule magnet; Single crystal X-ray analysis; Mn_{12} complexes; a.c. and d.c. magnetic susceptibility; 2-Thiophenecarboxylic acid; PPh_4 salt

1. Introduction

A 12-nuclei manganese complex $[Mn_{12}O_{12}(OAc)_{16}(H_2O)_4]$ (Mn_{12}-ac) is the firstly discovered and the most extensively studied SMM [1–4]. It is well known that the bridging $CH_3CO_2^-$ ligands of Mn_{12}-ac can be replaced by other carboxylates, such as substituted acetates or substituted benzoate, to afford various $[Mn_{12}]$ derivatives [5,6]. However, those carboxylates have no functional groups to coordinate to other metal ions except for the bridging CO_2^- group. If the carboxylate ligands have additional functional groups to coordinate to other metal ions, we can assemble them through the coordination bonds to form dimmers, oligomers and/or polymers of $[Mn_{12}]$ complexes. The important point is that the coordination ability of the additional functional group should be weaker than that of the bridging CO_2^- group, otherwise the $[Mn_{12}]$ structure cannot be retained during a ligand-exchange reaction. We chose thiophenecarboxylic acid for this purpose [7]. Here, we report the synthesis and magnetic susceptibility of a $[Mn_{12}]$ complex substituted by 2-thiophenecarboxylic acids (tpcH) and its tetraphenylphosphonium salt.

2. Experimental

2.1. Compound preparation

All chemicals and solvents were used as received; all preparations and manipulations were performed under

* Corresponding author. Tel.: +81-66721-2332; fax: +81-66723-2721.
E-mail address: kuroda@chem.kindai.ac.jp (T. Kuroda-Sowa).

0277-5387/03/$ - see front matter
doi:10.1016/S0277-5387(03)00184-0

argon atmosphere using Schlenk techniques. The Mn_{12}-ac was prepared by the literature method [8].

2.2. $[Mn_{12}O_{12}(O_2CC_4H_3S)_{16}(H_2O)_4]$ (1)

To a slurry of Mn_{12}-ac (600 mg, 0.32 mmol) in CH_2Cl_2 (100 ml) was added a large excess of tpcH (1.2 g, 9.64 mmol). The mixture was stirred overnight in a closed flask and filtered to remove any undissolved solid. Hexane was added to the filtrate until precipitation of a dark brown solid was observed. The resulting solid was collected by filtration and the above treatment was repeated twice. Recrystallization from CH_2Cl_2–hexane gave microcrystals of **1**. The yield was 88%. Anal. Calc. for $C_{81}H_{58}Cl_2Mn_{12}O_{48}S_{16}$ (as $\mathbf{1}\cdot CH_2Cl_2$): C, 31.98; H, 1.92; N, 0.00. Found: C, 31.96; H, 1.92; N, 0.00%.

2.3. $[PPh_4][Mn_{12}O_{12}(O_2CC_4H_3S)_{16}(H_2O)_2]$ (2)

To a stirred dark brown solution of complex **1** (100 mg, 0.034 mmol) in CH_2Cl_2 (10 ml) was added solid PPh_4I (15.8 mg, 0.034 mmol). The solution was stirred for 45 min. The resultant solution was filtered to remove any undissolved solid. To the filtrate a mixture of CH_2Cl_2–hexane and pure hexane were successively added slowly. After 3 days, black crystals suitable for X-ray analysis were obtained. Anal. Calc. for $C_{105}H_{80}Cl_2Mn_{12}O_{49}PS_{16}$ (as $\mathbf{2}\cdot CH_2Cl_2\cdot H_2O$): C, 37.49; H, 2.28; N, 0.00. Found: C, 37.66; H, 2.36; N, 0.00%.

2.4. Physical measurements

Direct current (d.c.) and alternating current (a.c.) magnetic susceptibility data were collected on microcrystalline or a single-crystal sample restrained in eicosane to prevent torquing on a Quantum Design MPMS2 or MPMS7 SQUID magnetometer equipped with a 1 or 7 T magnet and capable of achieving temperatures of 1.7–400 K. A diamagnetic correction to the observed susceptibilities was applied using Pascal's constants. The magnitude of a.c. field was fixed to 0.3 mT, oscillating at a frequency in the range 5–997 Hz.

2.5. X-ray structure analysis

Diffraction data for **2** was collected at −163 °C on a Rigaku/MSC Mercury CCD area detector with Rigaku AFC7 diffractometer equipped with graphite monochromated Mo Kα radiation. Crystal data and details of measurements for **2** are summarized in Table 1. The structure was solved by direct method and expanded using Fourier techniques. The non-hydrogen atoms were refined either anisotropically or isotropically by full-matrix least-squares calculations. Due to disordering of thiophene rings, we could not distinguish a sulfur atom and a carbon atom in 3-position in each thiophene ring. During the refinement, they are all treated as sulfur atoms with somewhat low occupancies, with a constraint of their total occupancy equal to 1.37. Hydrogen atoms were not included. Reliability factors are defined as $R_1 = \Sigma||F_o|-|F_c||/\Sigma|F_o|$?and $wR_2 = \{\Sigma w(|F_o|-|F_c|)^2/\Sigma w|F_o|^2\}^{1/2}$. The final R_1 and wR_2 values are also listed in Table 1.

Table 1
Crystallographic data for **2**

Complex	**2**
Formula	$C_{107}H_{78}Cl_6Mn_{12}O_{47}P_1S_{16}$
M	3531.67
Color, habit	black, brock
Crystal size (mm)	$0.5 \times 0.4 \times 0.3$
Space group	$P\bar{1}$ (No. 2)
T (°C)	−163
Unit cell dimensions	
a (Å)	16.584(2)
b (Å)	18.557(4)
c (Å)	23.026(3)
α (°)	97.097(8)
β (°)	91.463(5)
γ (°)	99.674(8)
V (Å^3)	6924(1)
Z	2
ρ_{calc} (g cm^{-3})	1.694
Radiation, λ (Å)	Mo Kα (0.7109)
μ (cm^{-1})	1.502
R_1 [a], wR_2 [b]	0.1076, 0.3529

[a] $R_1 = \Sigma||F_o|-|F_c||/\Sigma|F_o|$.
[b] $wR_2 = \{\Sigma w(|F_o|-|F_c|)^2/\Sigma w|F_o|^2\}^{1/2}$.

3. Results and discussion

3.1. Crystal structure of $[PPh_4][Mn_{12}O_{12}(O_2CC_4H_3S)_{16}(H_2O)_2]\cdot\mathbf{3}\cdot CH_2Cl_2\cdot H_2O$ ($\mathbf{2}\cdot\mathbf{3}\cdot CH_2Cl_2\cdot H_2O$)

A molecular core structure of **2** is shown in Fig. 1 together with the numbering scheme for some selected atoms. The anionic Mn_{12} moiety is similar to the usual Mn_{12} complex except that there are only two water molecules coordinated. The central cubane structure consists of four Mn^{IV} ions and four μ^3-bridging O^{2-} ions, which is surrounded by eight peripheral Mn ions and eight μ^3-bridging O^{2-} ions. The other coordination sites of manganese ions are occupied by eight axial and eight equatorial μ^2-bridging tpc anions and by two water molecules. There are two five-coordinated Mn ions: Mn(6) and Mn(10) ions. All Mn–O bond lengths around Mn(6) are greater than 2.0 Å, which implies that Mn(6) ion has the oxidation state of +2. On the other hand, those of Mn(10) are divided into two groups: four shorter bonds less than 2.0 Å and one longer than 2.0 Å, which implies Jahn–Teller distortion

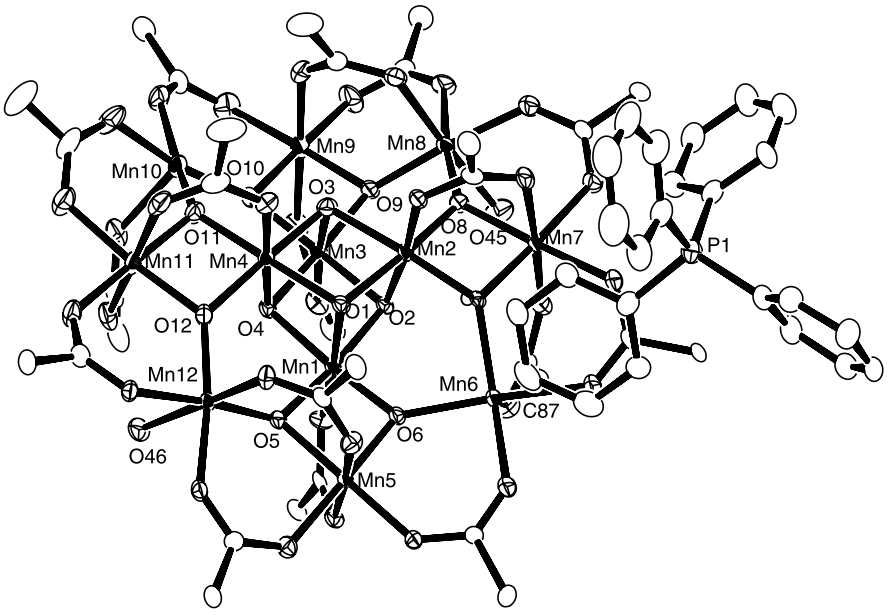

Fig. 1. An ORTEP drawing of a molecular structure of complex **2**. Atoms consisting of the $Mn_{12}O_{12}$ core, two water oxygen atoms and a phosphorous atom are numbered. Thiophene rings and hydrogen atoms are omitted for clarity.

on a Mn^{+3} ion. The oxygen atom involved in the longer Mn–O bond comes from the axial bridging tpc, indicating that Jahn–Teller axis is roughly parallel to the axial direction. Similar considerations on the rest of the peripheral Mn ions clearly indicate that all of Jahn–Teller axes are roughly parallel to each other.

In the previous papers on the one-electron reduced $[Mn_{12}]$ complexes of $[PPh_4][Mn_{12}O_{12}(O_2CEt)_{16}(H_2O)_4]$ [6] and $[Co(C_5Me_5)_2][Mn_{12}O_{12}(O_2CC_6F_5)_{16}(H_2O)_4]$ [9], the reduction site was assigned to one of Mn^{III} ions on the basis of the bond valence sum analysis. A bond valence sum [10] is an empirical value, based on crystallographically determined metal–ligand bond distances, that may be used to determine the oxidation state of a metal. Bond valence sums (s) were calculated using Eq. (1),

$$s = \exp\left[\frac{r_0 - r}{B}\right] \quad (1)$$

where r is the observed bond length, and r_0 and B the empirically determined parameters. Values for r_0 are tabulated for Mn^{n+} ($n = 2, 3, 4$) [10].

On the basis of the valence bond sum analysis for **2** shown in Table 2, it is clear that four Mn ions in the central cubane have +4 oxidation states while all the peripheral Mn ions except for Mn(6) ion have +3 oxidation states. Mn(6) ion has clearly a +2 oxidation state as expected. This indicates that the additional electron is trapped at Mn(6) ion to form a mixed valence $Mn^{II}Mn_7^{III}Mn_4^{IV}$ state. The reduction at a Mn^{III} ion not at a Mn^{IV} ion is similar to previous results [6,9].

As can be seen from Fig. 1, a phenyl carbon C(87) of the tetraphenylphosphonium cation is located in the vicinity of the vacant site of Mn(6) ion (Mn(6)–C(87) = 3.363(7) Å). If a phenyl hydrogen atom is located at an ideal position with a C–H bond length of 0.95 Å, the Mn(6)–H distance becomes 2.9 Å and the position is almost near the *trans* to the O(39) atom (angle: O(39)–Mn(6)–H = 170.8°). Although the length is larger than the Mn–H distance observed in $HMn(CO)_5$ (1.576 Å) [11], it is still shorter than the sum of van der Waals radii (3.2 Å). It is suggested that there is a certain Coulomb interaction between them because the anionic charge of the Mn_{12} complex resides at the Mn(6) ion and the C(87) carbon is a part of the cation.

Another interesting feature of **2** is the existence of the π–π interaction between thiophene rings. Fig. 2 shows a

Table 2
Bond valence sums for each Mn atom in complex **2** assuming various charges [a]

Atom	Mn^{2+}	Mn^{3+}	Mn^{4+}
Mn(1)	4.439	4.093	*4.017*
Mn(2)	4.421	4.077	*4.000*
Mn(3)	4.422	4.077	*4.001*
Mn(4)	4.431	4.086	*4.009*
Mn(5)	3.492	*3.220*	3.160
Mn(6)	*2.227*	2.054	2.015
Mn(7)	3.368	*3.105*	3.047
Mn(8)	3.415	*3.149*	3.090
Mn(9)	3.558	*3.281*	3.219
Mn(10)	3.402	*3.137*	3.078
Mn(11)	3.496	*3.223*	3.163
Mn(12)	3.493	*3.221*	3.161

[a] The italicized value is the one closest to the actual charge for which it was calculated. The oxidation state of a particular atom can be taken as the nearest whole number to the italicized value.

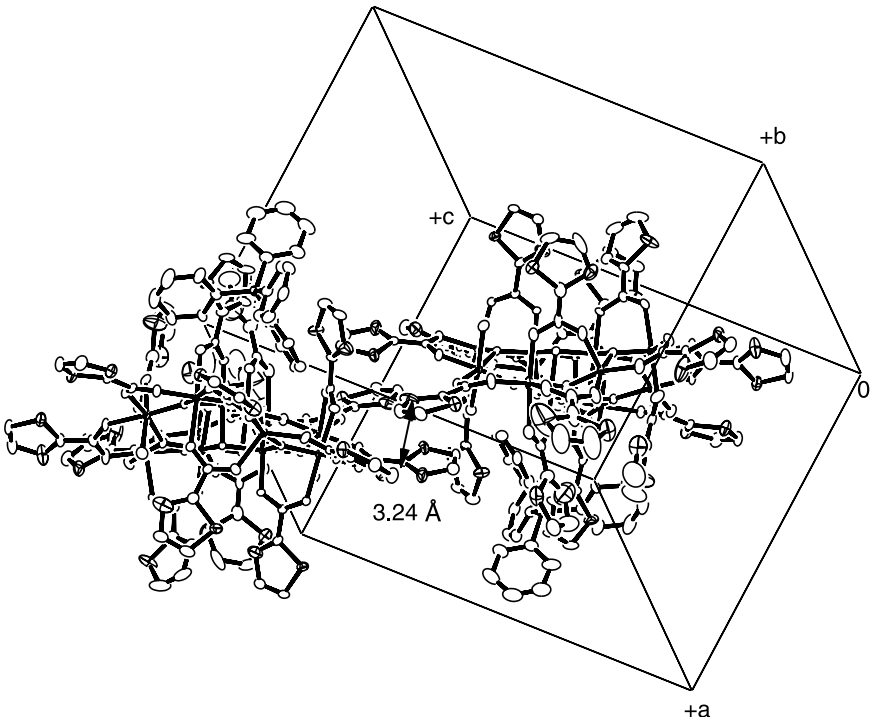

Fig. 2. An ORTEP drawing of crystal packing of **2**. Hydrogen atoms and solvent molecules incorporated into a crystal are omitted for clarity.

molecular packing view of two neighboring molecules. The equatorial thiophene rings of each molecule have π–π interaction with S···C or S···S contacts ranging from 3.24 to 3.6 Å. The π–π interaction expands not only to the equatorial direction but also to the axial one. Although the influence of these π–π interactions to the SMM behavior is not clear, the interaction between SMMs is important for realizing the future memory devices using SMMs [12].

3.2. Magnetic properties of *1* and *2*

The d.c. magnetization of **1** and **2** were measured from 4 to 280 K at 1.0 T and results are shown in Fig. 3. As temperature increases, the $\chi_M T$ value of **1** showed a maximum of 53.1 cm^3 K mol^{-1} at 12 K and a broad minimum of 18.0 cm^3 K mol^{-1} at around 160–180 K and again increases slightly to 19.5 cm^3 K mol^{-1} at 280 K. The large $\chi_M T$ maximum at low temperature is consistent with $S = 10$ if the g-value equals to 1.93. For the complex **2**, the similar behavior was observed: a maximum of 52.0 cm^3 K mol^{-1} at around 12 K and a broad minimum of 18.5 cm^3 K mol^{-1} at around 160–180 K and again increases slightly to 20.8 cm^3 K mol^{-1} at 280 K. In order to estimate the ground spin state (S) and the magnitude of the zero-field splitting (D) of **2**, d.c. magnetization data were collected in the tempera-

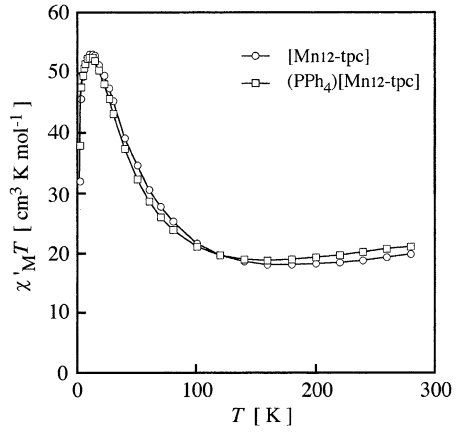

Fig. 3. Plots of $\chi_M T$ vs T for polycrystalline samples of **1** and **2** measured by d.c. susceptibility.

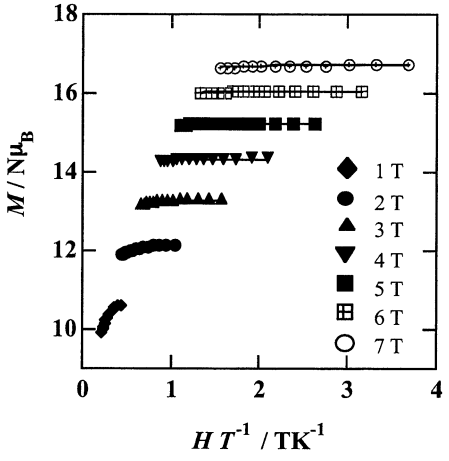

Fig. 4. Reduced magnetization data for **2** with different external field. Lines show the best fit assuming $S = 19/2$, $g = 1.99$ and $D = -0.61$ K.

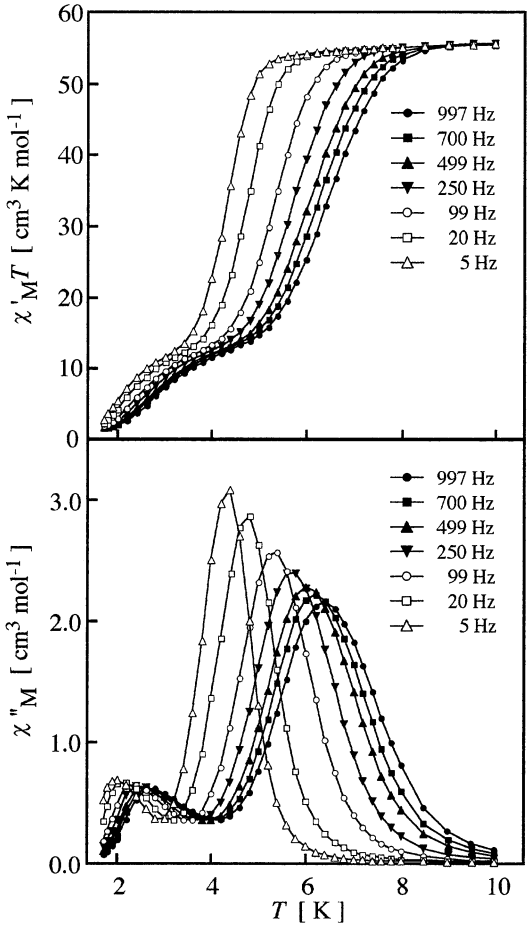

Fig. 5. Plots of $\chi'_M T$ vs T (top) and χ''_M vs T (bottom) for a polycrystalline sample of complex **1** in a 0.3 mT a.c. field oscillating at the indicated frequencies, where χ'_M and χ''_M are the in-phase and the out-of-phase magnetic susceptibilities, respectively.

ture range 1.9–4.5 K and at external fields of 1.0–7.0 T for polycrystalline sample of complex **2**. The sample was restrained in eicosane matrix to prevent torquing at high fields. The observed magnetization data $M/(N\mu_B)$ were plotted vs H/T in Fig. 4, which were fitted with a magnetization fitting program "axfit" [13] assuming an $S = 19/2$ ground state. The lines in Fig. 4 show the fitting with the parameters of $g = 1.99$ and $D = -0.61$ K.

In order to investigate the dynamic behavior of the magnetic moment, a.c. magnetic susceptibility of **1** and **2** were measured. Figs. 5 and 6 show plots of $\chi'_M T$ vs T (top) and χ''_M vs T (bottom) for complexes **1** and **2**, respectively, where χ'_M and χ''_M are the in-phase and out-of-phase a.c. susceptibilities, respectively. The $\chi'_M T$ values of **1** and **2** at 10 K are 55.5 and 51.9 cm^3 K mol^{-1}, respectively, which showed fairly good agreement to those obtained from d.c. susceptibility measurement. As temperature decreases, these values start to decrease at certain temperature depending on frequency. The decrease of $\chi'_M T$ value corresponds to the appearance of out-of-phase signal (χ''_M). The χ''_M values of **1** showed two peaks for each a.c. frequency, one in 4–6 K range and the other in 2–3 K range, which are corresponding to the high-temperature (HT) and the low-temperature (LT) phases, respectively, with the former being dominant. Those of **2**, on the other hand, showed only one peak between 3 and 5 K. Since the $\chi'_M T$ value of **2** at 1.7 K is not zero and the χ''_M values still keep on increasing with decreasing temperature down to 1.7 K, there should be another peak below 1.7 K corresponding to the LT phase, although its contribution is rather small compared to **1**. Therefore, the χ''_M peak observed between 3 and 5 K is assigned to the HT phase of anionic Mn_{12} complex **2**.

The frequency dependence of the χ''_M peak temperature can be analyzed by the Arrhenius law. On the basis of the plots of the natural logarithm of the relaxation time τ evaluated from $1/(2\pi\nu)$, where ν is the a.c. frequency, vs the inverse of the χ''_M peak temperature T, the effective energy barrier U_{eff} and pre-exponential factor τ_0 can be estimated by the following equation [14]:

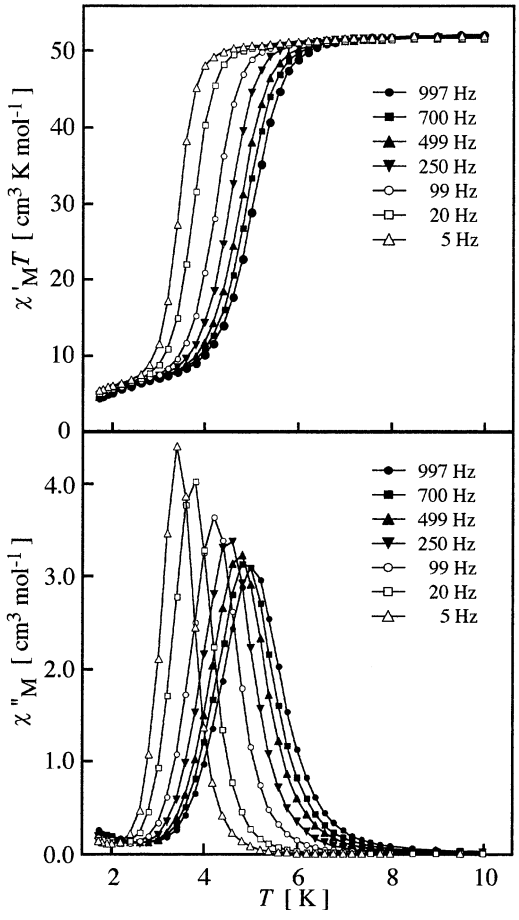

Fig. 6. Plots of $\chi'_M T$ vs T (top) and χ''_M vs T (bottom) for a polycrystalline sample of complex **2** in a 0.3 mT a.c. field oscillating at the indicated frequencies, where χ'_M and χ''_M are the in-phase and the out-of-phase magnetic susceptibilities, respectively.

Table 3
Pre-exponential factor τ_0 and the effective energy barrier U_{eff} estimated from Arrhenius plots for complexes **1** and **2**

Complex	Phase	τ_0 (s)	U_{eff} (K)
1	LT	1.6×10^{-10}	39.6
1	HT	3.8×10^{-9}	69.1
2	HT	1.9×10^{-9}	57.1

$$\tau = \tau_0 \exp\left(\frac{U_{eff}}{k_B T}\right) \quad (2)$$

where k_B is the Boltzmann constant. The Arrhenius plots for **1** and **2** are shown in Fig. 7. The solid lines show the results of least-squares fits of the a.c. susceptibility relaxation data to Eq. (2). The effective energy barrier U_{eff} and pre-exponential factor τ_0 are determined as shown in Table 3. The effective energy barriers U_{eff} for HT phases were evaluated to be 69 and 57 K for **1** and **2**, respectively. The former is somewhat smaller than that obtained for the neutral complex $[Mn_{12}O_{12}(NO_3)_4(O_2CCH_3)_{12}(H_2O)_4]$ (72 K [15]) and the latter is comparable to those of anionic $[Mn_{12}]^-$ SMMs such as $[PPh_4][Mn_{12}O_{12}(O_2CEt)_{16}(H_2O)_4]$ (60.2 K [16]) and $[PPh_4][Mn_{12}O_{12}(O_2CPh)_{16}(H_2O)_4]$ (55 K [17]; 57.5 K [18]). The latter is also comparable to the value of $(S^2-1/4)|D|$ ($=54.9$ K) estimated from the reduced magnetization fitting. At 997 Hz a.c. frequency, the anionic complex **2** shows χ''_M peak at 5.0 K while the parent neutral complex **1** shows a χ''_M peak at 6.5 K. The lower temperature shift of the χ''_M peak on one-electron reduction has been also observed for other Mn_{12} complexes [9].

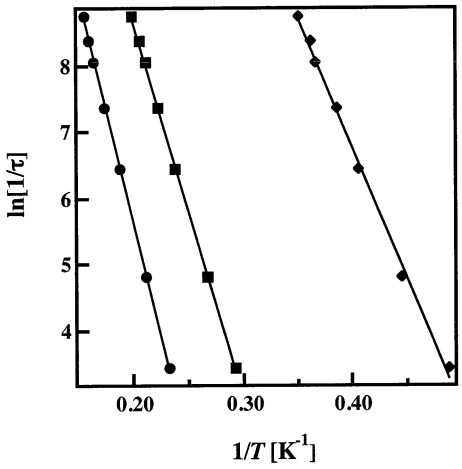

Fig. 7. Plots of the natural logarithm of the inverse of the magnetization relaxation time $\ln(1/\tau)$ vs the inverse of the absolute temperature of χ''_M peaks for the HT phase of **1** (●), the LT phase of **1** (◆) and the HT phase of **2** (■). The solid lines represent least-squares fits of the data to the Arrhenius equation (see the text).

4. Conclusion

We have synthesized two novel Mn_{12} complexes with thiophenecarboxylate bridges, **1** and **2**, which showed SMM behavior on a.c. susceptibility. The crystal structure determination of tetraphenylphosphonium salt (**2**) revealed that there are only two water molecules coordinated to Mn ions. By means of the valence bond sum analysis the reduction site was determined to be the Mn(6) ion and **2** has the mixed valence state Mn^{II}-Mn_7^{III} Mn_4^{IV}.

5. Supplementary material

Crystallographic data for the structural analysis have been deposited with the Cambridge Crystallographic Data Centre, CCDC No. 194476. Copies of this information may be obtained free of charge from The Director, CCDC, 12 Union Road, Cambridge, CB2 1EZ, UK (fax: +44-1233-336033; e-mail: deposit@ccdc.cam.ac.uk or www: http://www.ccdc.cam.ac.uk).

Acknowledgements

This work was supported in part by a Grant-in-Aid for Science Research from the Ministry of Education, Science and Culture, Japan. The authors are grateful to Kinki University for the financial support.

References

[1] E.M. Chudnovsky, Science 274 (1996) 938.
[2] B. Schwarzschild, Phys. Today 17 (1997).
[3] J.R. Friedman, M.P. Sarachik, J. Tejada, R. Ziolo, Phys. Rev. Lett. 76 (1996) 3830.
[4] R. Sessoli, D. Gatteschi, A. Caneschi, M.A. Novak, Nature 365 (1993) 141.
[5] R. Sessoli, H.-L. Tsai, A.R. Schake, S. Wang, J.B. Vincent, K. Folting, D. Gatteschi, G. Christou, D.N. Hendrickson, J. Am. Chem. Soc. 115 (1993) 1804.
[6] H.J. Eppley, H.-L. Tsai, N.D. Vries, K. Folting, G. Christou, D.N. Hendrickson, J. Am. Chem. Soc. 117 (1995) 301.
[7] T. Kuroda-Sowa, T. Nogami, M. Maekawa, M. Munakata, Mol. Cryst. Liq. Cryst. 379 (2002) 179.
[8] T. Lis, Acta Crystallogr. Sect. B B36 (1980) 2042.
[9] T. Kuroda-Sowa, M. Lam, A.L. Rheingold, C. Frommen, W.M. Reiff, M. Nakano, J. Yoo, A.L. Maniero, L.-C. Brunel, G. Christou, D.N. Hendrickson, Inorg. Chem. 40 (2001) 6469.
[10] I.D. Brown, D. Altermatt, Acta Crystallogr. Sect. B 412 (1985) 244.
[11] E.A. McNeill, F.R. Scholer, J. Am. Chem. Soc. 99 (1977) 6243.
[12] W. Wernsdorfer, N. Aliaga-Alcalde, D.N. Hendrickson, G. Christou, Nature 416 (2002) 406.

[13] J. Yoo, A. Yamaguchi, M. Nakano, J. Krzystek, W.E. Streib, L.-C. Brunel, H. Ishimoto, G. Christou, D.N. Hendrickson, Inorg. Chem. 40 (2001) 4604.
[14] S.M.J. Aubin, M.W. Wemple, D.A. Adams, H.-L. Tsai, G. Christou, D.N. Hendrickson, J. Am. Chem. Soc. 118 (1996) 7746.
[15] P. Artus, C. Boskovic, J. Yoo, W.E. Streib, L.-C. Brune, D.N. Hendrickson, G. Christou, Inorg. Chem. 40 (2001) 4199.
[16] S.M.J. Aubin, S. Spagna, H.J. Eppley, R.E. Sager, G. Christou, D.N. Hendrickson, J. Chem. Soc., Chem. Commun. (1998) 803.
[17] K. Takeda, K. Awaga, Phys. Rev. B 56 (1997) 14560.
[18] S.M.J. Aubin, Z. Sun, L.A. Pardi, J. Krzystek, K. Folting, L.-C. Brunel, A.L. Rheingold, G. Christou, D.N. Hendrickson, Inorg. Chem. 38 (1999) 5329.